Investigational New Drugs (2019) 37:948–960
https://doi.org/10.1007/s10637-018-00717-9

PRECLINICAL STUDIES

# Sensitization of colorectal cancer to irinotecan therapy by PARP inhibitor rucaparib

Titto Augustine[1] · Radhashree Maitra[2] · Jinghang Zhang[3] · Jay Nayak[2] · Sanjay Goel[1,2]

Received: 9 November 2018 / Accepted: 19 December 2018 / Published online: 5 January 2019


## Summary

Intended to explore synthetic lethality and develop better combinatorial regimens, we screened colorectal cancer (CRC) cells using poly ADP-ribose (PAR) polymerase (PARP) inhibitors and cytotoxic agents. We studied four PARP inhibitors and three DNA-damaging agents, and their combinations using sulforhodamine B assay. Rucaparib demonstrated the greatest synergy with irinotecan, followed by olaparib and PJ34. Rucaparib and irinotecan was further subjected to detailed examination to determine combination index (CI) and underlying mechanism of action. Effectiveness and sequence dependence of this combination were assessed in microsatellite stable (MSS) and unstable (MSI) CRC and HCT116 isogenic cell lines. The degree of cell cycle arrest and apoptosis was determined by FACS. In vivo studies were performed to confirm efficacy of this combination. PAR levels in MSI and PARP expression in MSI and MSS cell lines were diminished upon combinatorial treatment. HCT116 isogenic cells revealed the importance of p21, p53 and PTEN in exerting synergy. In MSI cells, administration of rucaparib prior to irinotecan enhanced cytotoxicity compared to other strategies explored. FACS revealed S-phase arrest and increased late-stage apoptosis in MSS, and G2-M arrest and total and early-stage apoptosis in MSI cells. In in vivo murine xenograft models, a significant reduction in tumor volume and expression of Ki67, pancytokeratin and RPS6KB1, and increase in expression of caspase 3 were observed with the combination. In conclusion, among the various combinations studied, rucaparib plus irinotecan was the most synergistic one. Alterations in cell cycle arrest and apoptosis were dependent on MSI status in CRC cells.

**Keywords** PARP · Rucaparib · Irinotecan · Colorectal cancer · Combinatorial · Synergy

## Introduction

Overall survival for patients with metastatic colorectal cancer (CRC) has improved over the past decade. Current chemotherapeutic regimens for CRC include drugs that result in DNA damage via different mechanisms. Oxaliplatin causes the formation of DNA adducts, while irinotecan blocks re-ligation of DNA strands by inhibiting topoisomerase 1 [1]. These two agents are often given in combination with the nucleotide analog 5-fluorouracil, an irreversible competitive inhibitor of thymidylate synthase that results in incorporation of metabolites into DNA [2]. Although these treatments are initially effective, all patients eventually develop resistance. The current 5-year survival rate for CRC is still 11%, partly due to the development of resistance over the course of treatment [3]. A major cause of drug resistance is increased DNA damage repair (DDR) [4].

During the process of continuous replication, cancer cells undergo DNA damage, which activates key proteins, including BRCA and poly ADP-ribose (PAR) polymerase (PARP) that repair this damage [5]. PARP1 has high affinity for single- and double-stranded DNA breaks and thought to play a role in base excision repair. PARP1 binds tightly to DNA-strand breaks and following auto–poly ADP-ribosylation, is released, gaining access to the damaged DNA [6]. PARP inhibitors (PARPi), either alone or in combination with cytotoxic drugs, are utilized for BRCA1/2 mutated breast cancer [7]. Similarly, p53-deficient breast cancer cells treated with

✉ Sanjay Goel
sgoel@montefiore.org

[1] Department of Medicine, Albert Einstein College of Medicine, Bronx, NY 10461, USA

[2] Department of Medical Oncology, Montefiore Medical Center, Bronx, NY 10461, USA

[3] Department of Microbiology & Immunology and Flow Cytometry Core Facility, Albert Einstein College of Medicine, Bronx, NY 10461, USA

PARPi have been shown to lose resistance to the apoptosis-promoting and clinically active antitumor agent anthracycline [8].

Currently, three distinct PARPi, namely olaparib, rucaparib and niraparib are USFDA-approved for use in patients with ovarian cancer [9]. Olaparib is also indicated in triple negative breast cancer [5]. Additionally, single agent and combination trials are ongoing for a number of additional indications [7, 10, 11]. The use of PARPi in the management of CRC is poorly defined. No studies to date have demonstrated a significant reduction of CRC tumor growth by specific PARPi when combined with standard chemotherapeutic agents. The complexity of the genetic underpinnings of CRC may explain the limited activity of PARPi observed thus far in this disease. While ~84% of sporadic tumors show chromosomal instability, 13–16% exhibit hypermutation and demonstrate a microsatellite instability (MSI) phenotype due to defective DNA mismatch repair (MMR) [12]. Mismatch repair-proficient tumors include those that are microsatellite stable (MSS) or MSI-low [13]. For this study, we hypothesized that concurrent treatment of CRC cells with a DNA-damaging drug and a PARPi would be synergistic, potentially paving the way for more effective management of CRC. In addition, by utilizing "synthetic lethality", combinatorial treatment may provide added benefit in MSI-high CRC. In order to test our hypotheses, we used a collection of human CRC cell lines to identify the most synergistic PARPi and chemotherapeutic/cytotoxic drug combination and its mechanism of action. In addition, experiments were performed in MSI and MSS CRC cell lines to demonstrate efficacy in different genetic backgrounds. Finally, in vivo xenograft studies were performed to translate in vitro observations into a proof-of-concept pre-clinical treatment strategy.

## Materials and methods

### Drugs and chemicals

Oxaliplatin, irinotecan and 5-fluorouracil, obtained from Montefiore Medical Center outpatient pharmacy, were freshly prepared in deionized water/MEM media for each experiment. The PARP inhibitors olaparib and PJ34 were purchased from Selleck Chemicals (Houston, TX), veliparib from Cancer Therapy Evaluation Program (CTEP) (NCI, Bethesda, MD) and rucaparib from Clovis Oncology (San Francisco, CA). Olaparib, rucaparib and veliparib were dissolved in anhydrous DMSO (Sigma-Aldrich, St. Louis, MO) and PJ34 in water. All PARPi were kept as 10 mM stock solutions and stored at −20 °C. The following antibodies and concentrations were used for Western blotting: PARP-1 and p21–1:500 (Santa Cruz Biotechnology, Inc., Dallas, TX), γH2AX - 1:1000 (EMD Millipore, Billerica, MA) and β actin - 1:15,000 (Sigma-Aldrich). All other chemicals were of analytical grade and commercially available.

### Cell culture

The study was performed in parental HCT116 that harbors both activating KRAS ($KRAS^{G13D}$) and PIK3CA ($PIK3CA^{H1047R}$) mutations, and its isogenic derivatives including HCT116 $Bax^{-/-}$, HCT116 $p21^{-/-}$, HCT116 $p53^{-/-}$, HCT116 $PTEN^{-/-}$, HCT116 KRAS wt (Hke3) and HCT116 PIK3CA wt, along with LIM2405, HCT15, RKO (all are MSI), HT29, SW837 and Caco2 (all are MSS) human CRC cell lines. All parental cell lines were obtained from the American Type Culture Collection (ATCC, Manassas, VA). Isogenic HCT116 KRAS and PIK3CA wt and mutant cells were generously provided by the Sasuzaki and Vogelstein/Velculescu laboratories, respectively [14–16]. All cell lines were cultured in MEM supplemented with 10% fetal bovine serum, 1x antibiotic/antimycotic (100 units/ml streptomycin, 100 units/ml penicillin, and 0.25 μg/ml amphotericin B), 1x MEM Non-Essential Amino Acids Solution, and 10 mM HEPES buffer solution (all from Thermo Fisher Scientific, Waltham, MA). All lines were tested to be negative for mycoplasma contamination (Venor™GeM Mycoplasma Detection Kit, Sigma-Aldrich). Cell lines were authenticated by clustering analysis of genome-wide mRNA expression microarray data at the time of these experiments [17]. Cell lines were cultured until they reached 70–80% confluence.

### Cytotoxicity assay

After exposure to drugs or controls in 96-well plates, cell survival/proliferation was measured by a spectrophotometric dye incorporation assay using sulforhodamine B (SRB) [18]. Cells were fixed with trichloroacetic acid (Sigma-Aldrich) for 1 h, followed by staining for 30 min with 0.4% (wt/vol) SRB (Sigma-Aldrich) dissolved in 1% acetic acid. The number of viable cells was directly proportional to protein bound-dye, which was solubilized with 10 mM Tris base solution pH 10.5 and quantified by fluorometric ELISA at 540 nM (Bio-Rad, Hercules, CA; Microplate Reader). All experiments were performed in duplicate and repeated a minimum of three times. The $IC_{50}$ was assessed from the dose-response curves.

### Multiple drug effect analysis

1, 2 and 5 μM concentrations of PARPi (olaparib, rucaparib, PJ34 and veliparib) and 0.2 μM concentration of oxaliplatin or 0.5 μM concentration of either 5-fluorouracil or irinotecan were used to analyze combination strategies. During the second phase, various concentrations of irinotecan and rucaparib

were added in a fixed $IC_{50}$-based molar ratio (irinotecan: rucaparib) of 1:2 for HCT15, HCT116, HT29, LIM2405, RKO and SW837. All assays were done in duplicates. The mode of interaction (synergy, antagonism or additivity) was determined by calculating the CI [19] using CompuSyn software program (CompuSyn, Inc., Paramus, NJ). CI is a quantitative measure of the degree of drug synergy (CI 1 = additive effects), (CI < 1, synergy), (CI > 1, antagonism) [10].

## Protein extraction and Western blotting

Expression of PARP1, γH2AX, p21 and β-actin were determined by Western blotting. Cells were treated with specified concentrations of irinotecan and/or rucaparib for 24, 48 or 72 h prior to lysis in RIPA buffer (Cell Signaling Technology, Inc., Danvers, MA) containing 1 mM phenylmethanesulfonylfluoride (Sigma-Aldrich). Protein concentrations were determined with a bicinchoninic (BCA) protein assay (Thermo Fisher Scientific). Equal quantities of total protein were loaded and separated by 12% SDS-PAGE then transferred to a polyvinylidene difluoride membrane (Thermo Fisher Scientific). Next, blocking with 5% *w/v* non-fat dry milk or 5% w/v bovine serum albumin in Tris-buffered saline with 0.1% Tween 20 (TBST-T) was performed. The membranes were incubated overnight at 4 °C with relevant primary antibodies followed by incubation with horseradish peroxidase-conjugated secondary antibody (dilution, 1:10,000; GE Healthcare Bio-Sciences/Amersham, Pittsburg, PA) for 2 h at room temperature. Proteins were visualized using a Kodak Gel Logic 2200 imaging system (Kodak, Rochester, NY) with Luminata™ Crescendo Western HRP substrate (EMD Millipore, Billerica, MA, USA) [20].

## Determination of cellular PAR

Total cellular PAR levels were quantified using a commercially available PARP in vivo Pharmacodynamic Assay 2nd Generation (PDA II) Kit (4520–096-K; Trevigen Inc., Gaithersburg, MD) according to the manufacturer's instructions and as described previously [21]. Briefly, serially diluted PAR standards, diluted test samples, Jurkat cell lysate standards as positive controls and sample buffer (background control) were analyzed in triplicate. LIM2405 and SW837 cells ($10^6$) were seeded in 60 mm dishes and analyzed after 72 h of treatment. Dishes were placed on ice and lysed according to the kit protocol. After cell lysis and DNA digestion, total protein was quantified in each sample, and 10 μg of cell extracts were added to PAR-capture antibody pre-coated plates, which were covered with sealing film and incubated overnight at 4 °C. Wells were washed four times with PBS with Tween-20 (PBST), and PAR-detecting polyclonal antibody (1:250) was added at 25 °C for 2 h. Each well was again washed four times in PBST. HRP conjugate (1:250) was added at 25 °C for 1 h. After washing, goat anti-rabbit IgG-HRP conjugate was added at 25 °C for 1 h. Cells were washed four times and a 1:1 mixture of PARP PeroxyGlow A and B was added. Luminescence was measured using BMG LUMIstar Galaxy microplate reader. The validation criteria of the assay were met and double measurement was conducted to validate reliability of the assay. Units of measure were pg/mL PAR, normalized to 100 μg protein as determined with the BCA assay.

## Cell cycle analysis

Flow cytometric analyses of LIM2405 and SW837 were carried out using a BD LSR II machine (Becton Dickinson Immunocytometry Systems USA, San Jose, CA) after treatment in duplicate with control IgG1 (10 μg/ml; Calbiochem, San Diego, CA) or with 200 nM irinotecan and/or 400 nM rucaparib and combination for 24 h. To monitor DNA synthesis, determination of BrdU (Sigma-Aldrich) incorporation was performed using standard protocols. DNA was counterstained with 5μg/ml propidium iodide (PI) for at least 20 min before flow cytometric analysis [22].

## Apoptosis determination

This assay is based on the phosphatidylserine detection on the apoptotic cells surface, using fluorescently labeled annexin V in combination with the dead cell marker, PI [23]. LIM2405 and SW837 cells were treated in duplicate in 1 of 4 groups; control IgG1 (10 μg/ml; Calbiochem, San Diego, CA), 200 nM irinotecan, 400 nM rucaparib, and combination. After 3, 6, 12, 24 and 48 h of drug(s) treatment, cells were harvested, washed in PBS and fixed using 1x binding buffer. The cells were stained with annexin V-FITC and PI using Annexin V Apoptosis Detection kit and according to the manufacturer's instructions (eBioscience, San Diego, CA). The level of apoptosis was assessed by fluorescence-activated cell sorting analysis within 4 h of dye addition. We calculated the apoptotic ratio by identification of four populations: (i) live cells, not undergoing detectable apoptosis: Annexin V (−) and PI (−), (ii) early apoptotic cells: Annexin V (+) and PI (−), (iii) late apoptotic cells: Annexin V (+) and PI (+), and (iv) cells that died through non-apoptotic pathway – necrotic cells: Annexin V (−) and PI (+).

## In vivo xenograft experiments

All animal care and experimental procedures were performed in accordance with protocols approved by the Albert Einstein College of Medicine's Institutional Animal Care and Use Committee (IACUC). A total of $10^6$ HCT116 cells were suspended in 50 μl of serum-free media and mixed with an equal volume of Matrigel (BD Biosciences, Bedford, MA). The mixtures were injected subcutaneously into the dorsal

flanks of 8-week-old athymic nude mice [24], which were obtained from Jackson Laboratory (Bar Harbor, ME). After the tumors had grown to approximately 100mm$^3$, the mice were treated with irinotecan, rucaparib, irinotecan combined with rucaparib, or the control group ($n = 4$–6 for each group; experiments done in triplicate). Animals received intraperitoneal injections of 1.25mg/kg bodyweight of irinotecan in normal saline twice weekly, and 20mg/kg of rucaparib in 0.5% (*w*/*v*) methylcellulose, daily, for 3 weeks. The combined group received the same doses of both agents at the same frequency and duration. The non-treated control group received a mixture of sucrose solution and normal saline. Tumor volume was measured every 3 days using caliper and calculated as follows: volume = longest tumor diameter × (shortest tumor diameter)$^2$/2 [25]. Animals were euthanized and tumors were excised upon reaching 2 cm$^3$ size.

### Tissue microarray and immunohistochemistry analysis

To determine the expression of caspase 3, Ki67, pancytokeratin and RPS6KB1 in excised HCT116 xenografts, tissues were harvested, formalin fixed, and used to create a tissue microarray (TMA) for immunohistochemistry [26]. TMA provide an opportunity to detect tissues on a large scale in a consistent manner. The process was as follows: TMA slides were deparaffinized twice with xylene for 5 min each, then sequentially transferred through 100%, 95%, 85%, 75% alcohol. Then, antigen recapture was performed on tissue sections using microwave treatment in 10 mmol/L sodium citrate buffer (pH 6.0) for 10 min. Immunohistochemistry was performed using the Cell and Tissue Staining Kit (R&D Systems, Inc., Minneapolis, MN). The sections were incubated overnight at 4 °C with anti-caspase 3 (1:400 dilution, ab2302, Abcam, Cambridge, MA), anti-pancytokeratin (1:200 dilution, ab27988, Abcam), and anti-RPS6KB1 (1:200 dilution, LS-C96584, LifeSpan Biosciences, Inc., Seattle, WA). TMA slides stained with PBS served as the controls. 3,3′-diaminobenzidine with hematoxylin was employed for counter stain. The slides were examined using an inversion fluorescence microscope (Olympus IX-71, Tokyo, Japan).

### Statistical analysis

Data were expressed as mean values ± SEM. As appropriate for the experimental design, statistical analysis was conducted using an unpaired *t*-test, or one-way analysis of variance (ANOVA) with post hoc test. A minimal level of statistical significance for differences in values was considered to be $p < 0.05$ and is indicated with an '*'. Data was analyzed with Excel (Microsoft) and GraphPad Prism®
Version 7.0 (GraphPad Software Inc.).

## Results

### Effects of cytotoxic drugs combined with PARP inhibitors on CRC cell growth

Oxaliplatin, 5-fluorouracil and irinotecan, as well as the small molecule PARPi olaparib, rucaparib, PJ34 and veliparib were tested as single agents for their effects on growth of CRC cell lines. The additive, synergistic or antagonistic effects of these drug combinations were analyzed by combining them in different molar ratios and for varying durations (Fig. 1a, heat map). Based on the percentage difference from additive effect, irinotecan and rucaparib exhibited the most synergistic growth inhibition. In contrast, oxaliplatin and veliparib had an antagonistic effect on cell growth.

The irinotecan rucaparib combination was further investigated. Result of CompuSyn analysis and CI values for six CRC cell lines are presented in Fig. 1b. Strikingly, synergistic antiproliferative effects (CI < 1) were observed in all except for ED75 and ED90 of SW837, an MSS cell line. Significant synergy (CI < 0.5) was observed in HCT116 and RKO. The CI values for $ED_{50}$ and $ED_{90}$ in cell lines are as follows: HCT15, 0.79–0.93; HCT116, 0.08–0.35; HT29, 0.57–0.96; LIM2405, 0.51–0.98; RKO, 0.38–0.39 and SW837, 0.75–111.8. As irinotecan in combination with rucaparib exhibited the most synergistic cytotoxic effect, further in-depth analyses were performed using this combination only.

### Viability check of single-agent and combinatorial treatment

Irinotecan and rucaparib were tested individually or in combination in a number of CRC cell lines to determine the range of cytotoxicity. For these experiments four MSI cell lines, including HCT116, RKO, HCT15 and LIM2405, and two MSS CRC cell lines, including SW837 and HT29 were tested in the SRB assay. Results are shown for the representative cell lines RKO and HT29. As shown in Fig. 2, a spectrum of sensitivity to irinotecan and rucaparib were observed. RKO was more sensitive both to single-agent rucaparib treatment ($p < 0.05$) and combination therapy ($p = 0.04$) compared with HT29, which might be due to the MMR-deficiency status of RKO. A cytotoxic effect by irinotecan alone was observed at 200 nM, and for rucaparib at 400 nM after 48 h of treatment. These findings prompted us to select these concentrations for future experiments.

### Functional assessment of PARP inhibition in combination with irinotecan

PAR levels, PARP1 and γH2AX expression were defined as functional aspects of PARP inhibition (Fig. 3). Rucaparib 400 nM was administered for 3, 6, 12, 24 and 48 h as single

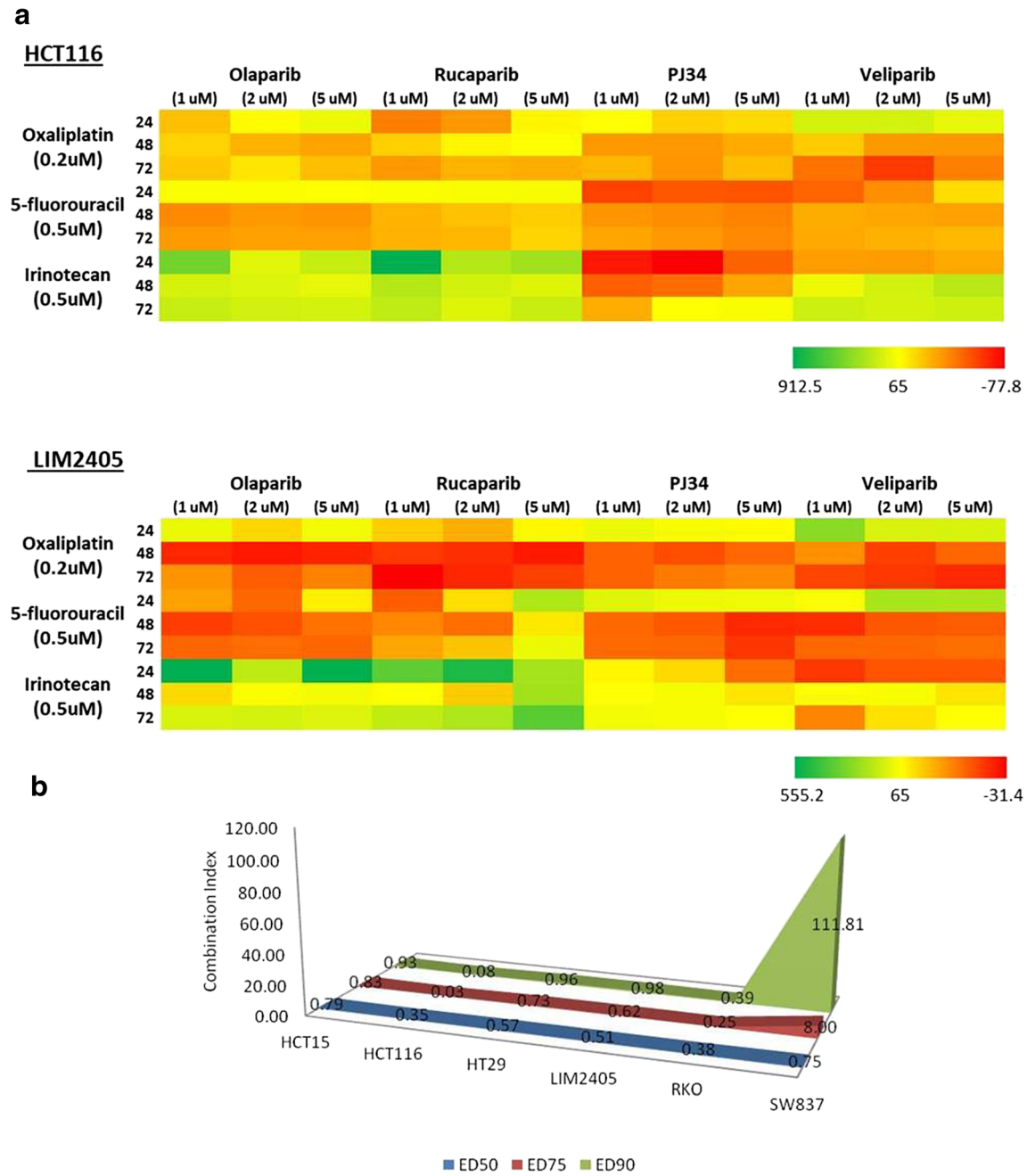


**Fig. 1 Drug interactions with PARPi. a** Heat maps represent additive, synergistic or antagonistic interactions of drugs and small molecule PARPi in CRC cell lines. Data correspond to percentage variation from additive effect of oxaliplatin, 5-fluorouracil and irinotecan with olaparib, rucaparib, PJ34 and veliparib. HCT116 and LIM2405 were treated with various concentrations and mixing ratios of these agents for 24, 48 and 72 h followed by SRB assay for cell viability [18]. Values ≥200 are considered as synergism (green blocks) and ≤ −20 is antagonism (red blocks). Combinations of irinotecan and rucaparib considered as most synergistic; combinations of irinotecan and PJ34, and oxaliplatin and veliparib considered as antagonistic [$n = 4$]. **b** Synergism was further demonstrated by CI analysis. Four MSI (HCT15, HCT116, LIM2405 and RKO) and two MSS (HT29 and SW837) CRC cell lines were subjected to varying but uniformly distributed concentrations of irinotecan and rucaparib for 24 h, and SRB assay done. CI was determination using CompuSyn v.1.0 at $ED_{50}$ (effective dose 50%), $ED_{75}$ and $ED_{90}$ [19]

agent and in combination with 200 nM of irinotecan. Rucaparib alone reduced PAR levels by ~25% in LIM2405 and ~70% in SW837 compared to untreated cells. Effects on PAR levels of the drug combination were more pronounced in the MSI cell lines compared to the MSS lines. Notably, administration of irinotecan as single agent increased PAR by 30–60% in LIM2405, perhaps due to the drug's increased potential to cause DNA damage and stress in an MSI context [27]. SW837 demonstrated two-fold endogenous PAR compared to LIM2405 (Fig. 3a).

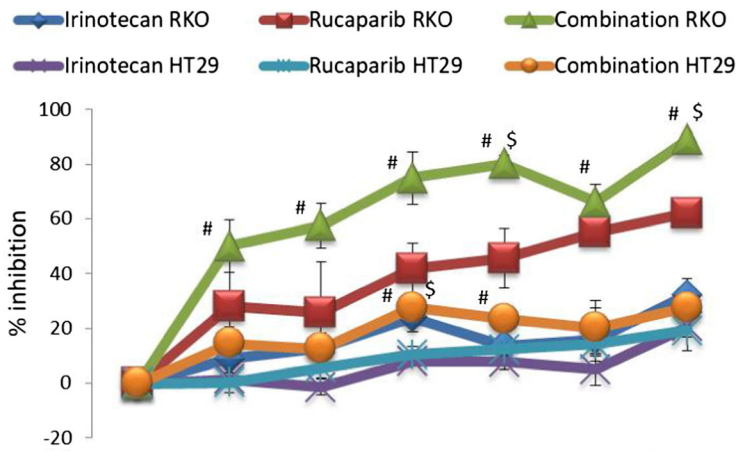


| Irinotecan (uM) | 0 | 0.05 | 0.1 | 0.2 | 0.5 | 0.75 | 1 |
|---|---|---|---|---|---|---|---|
| Rucaparib (uM) | 0 | 0.1 | 0.2 | 0.4 | 1 | 1.5 | 2 |
| Combination | 1 | 2 | 3 | 4 | 5 | 6 | 7 |

**Fig. 2 Dose ratio-dependent effects of irinotecan and rucaparib.** Representative MSI (RKO) and MSS (HT29) CRC cell lines were subjected to SRB assay for cell viability/growth inhibition 48 h post drug-addition. Each point on the plot corresponds to concentrations or combinations of drugs as mentioned in the table below chart – x axis representation. Combinatorial effect of irinotecan and rucaparib were highly synergistic ($p \leq 0.04$) and more pronounced in MSI than MSS ($p = \text{NS}$). '#' represents $p \leq 0.05$ compared to irinotecan single agent and '$' represents $p \leq 0.05$ compared to rucaparib single agent. Each point represents mean ± SEM of triplicate experiments

Expression of PARP1 and γH2AX was consistent with a response to DNA-damage. We measured protein levels of PARP1 in HCT116, LIM2405, SW837, RKO, and HT29 cell lines and the DNA double-strand breaks sensor, γH2AX, in all except SW837 by Western blot analysis (Fig. 3b) and quantified using the Image J software (NIH). When quantified and corrected for load (β-actin) the expression of PARP1 was increased by treatment with irinotecan in HCT116 and LIM2405, whereas rucaparib and combination downregulated it significantly ($p = 0.04$). γH2AX levels were upregulated by treatment with single agents and with combination therapy in LIM2405, and with irinotecan and combination therapy in the remaining three cell lines. Only HCT116 demonstrated a reduction in γH2AX level upon treatment with rucaparib.

## Efficacy of concurrent vs sequential administration of irinotecan and rucaparib

After establishing synergy between irinotecan and rucaparib treatment in vitro, subsequent studies were carried out to examine whether simultaneous versus sequential administration of irinotecan and rucaparib altered the efficacy of this combination (Fig. 4). Each drug was administered for 24 h. We found that concurrent administration of the drugs was more effective than sequential therapy. For sequential combinations, it was more effective to administer irinotecan before rucaparib. The exception was in HCT15 and SW837 cell lines, where administration of rucaparib followed by irinotecan was found to be more effective. MSI and MSS status were not determinants of efficacy of concurrent vs sequential treatments. However, administration of irinotecan followed by rucaparib proved to be less effective than concurrent treatment in all conditions (Fig. 4a).

Being prominent regulators of cell cycle, proliferation and apoptosis, we also analyzed role of Bax, KRAS, p21, p53, PI3-kinase and PTEN in relation to efficacy of concurrent vs sequential treatment (Fig. 4b and c). We used six isogenic cell lines derived from parental HCT116 and repeated the experiments as described above. For each cell line, except for the line carrying a p21 mutation, treatment with rucaparib prior to irinotecan increased the percentage of cell death compared to other treatment conditions (Fig. 4b). From these results we speculate that perhaps the absence of Bax, p21, p53 or PTEN caused antagonism upon simultaneous treatment of two drugs, or when irinotecan administered prior to rucaparib. In addition, in the presence of rucaparib, PARP activity and expression were reduced, which may have promoted responses to irinotecan via DNA-strand break-mediated cytotoxicity and cell death. Under all treatment conditions across the isogenic panel of cell lines, antagonism was more prominent in p21 mutants (Fig. 4c). These results suggested that p21, a cyclin-dependent kinase inhibitor and positive regulator of cell cycle arrest in presence of p53, was an important mediator of response to combination irinotecan and rucaparib.

To further examine the role of p21 and p53 in the response to combination irinotecan and rucaparib, we analyzed expression of p21 in p53 mutant and wt cells (Fig. 4d). While none of the treatments altered outcome in wt cells, p21 expression drastically increased upon combination treatment in p53 mutant HCT116. However, p53 wt LIM2405 also increased

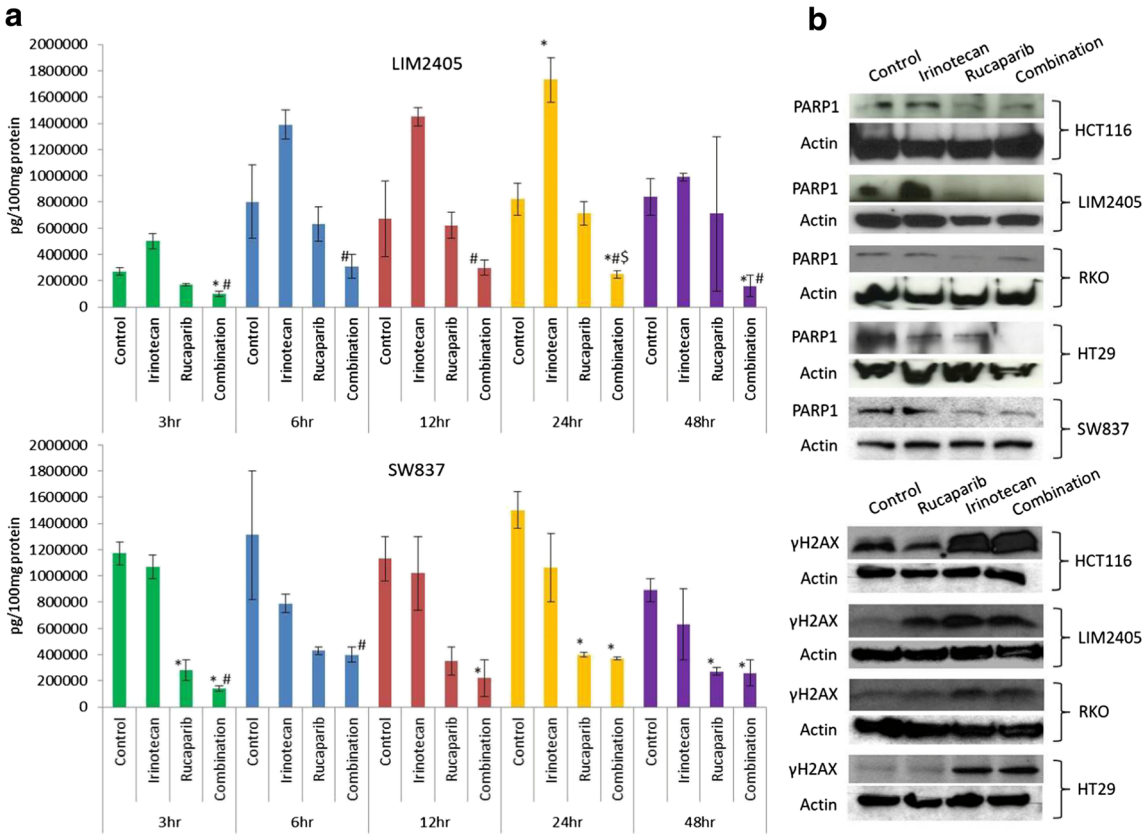


**Fig. 3 Measurement of PAR levels and expressions of PARP1 and γH2AX. a** PAR assay was performed using Trevigen's PARP in vivo Pharmacodynamic Assay 2nd Generation kit. PAR levels were reduced upon administration with 400 nM rucaparib single agent and in combination with 200 nM irinotecan. These experiments were repeated twice, and mean ± SD was plotted. **b** Expressions of PARP1 and γH2AX in CRC cell lines. Rucaparib alone and combination with irinotecan significantly reduced PARP1 in all cell lines tested. DNA damage sensor, γH2AX, was significantly increased ($p \leq 0.05$ compared to controls) upon treatment with irinotecan and its combination with rucaparib in all cell lines studied. These experiments were repeated twice. There was no significant difference in the expression of housekeeping protein β-actin

expression of p21 upon treatment with rucaparib and the combination, which was correlated with the synergistic effect of the two drugs on G2-M cell-cycle phase arrest (Fig. 5a). This prompted us to speculate that the initiation of cell death might be p21- and p53-dependent. p21 expression was significantly reduced after rucaparib treatment for 24 h in LIM2405 and p53 mutant of HCT116.

## Cell cycle perturbations and apoptosis in MSI and MSS cell lines

Cell cycle perturbations were analyzed by flow cytometry, after a 24 h of exposure to irinotecan and rucaparib in two CRC cells (Fig. 5a). In MSI cell line, LIM2405, treatment with irinotecan caused accumulation of cells in G2M, which was increased with the addition of rucaparib. Combination treatment reduced the fraction of cells in S phase to ~40% (Fig. 5b). In the MSS cell line, SW837, combination treatment induced significant accumulation of cells in S phase ($p = 0.03$) by reducing the number of cells in G0–1 peak. Although single-agent treatments also showed a similar trend, neither increase in S phase nor decrease in G0-G1 was significant.

We assessed the effect of two drugs to induce apoptosis over 3–48 h (Fig. 5c and d). The percentage of cells undergoing apoptosis increased upon duration of treatment. Combined treatment delayed apoptosis in SW836 compared to LIM2405. Except for the 3 h group, combination treatment significantly increased apoptosis in LIM2405. However, apoptosis was evident only at the 48 h treatment group in SW837 (data not shown). Noticeably, only LIM2405 demonstrated increased apoptosis after combination treatment. Levels of apoptosis upon single-agent treatment was indirectly proportional to combinatorial treatment (data not shown).

We further quantified stages of apoptosis in both cell lines under different treatment conditions and durations. Early-stage apoptotic cells were significantly increased in LIM2405, whereas late-stage apoptotic cells were increased in SW837 (Fig. 5d), particularly in the rucaparib single agent treated group (data not shown). In SW837, 48 h combinatorial treatment alone significantly increased late-stage apoptotic cells (Fig. 5d).

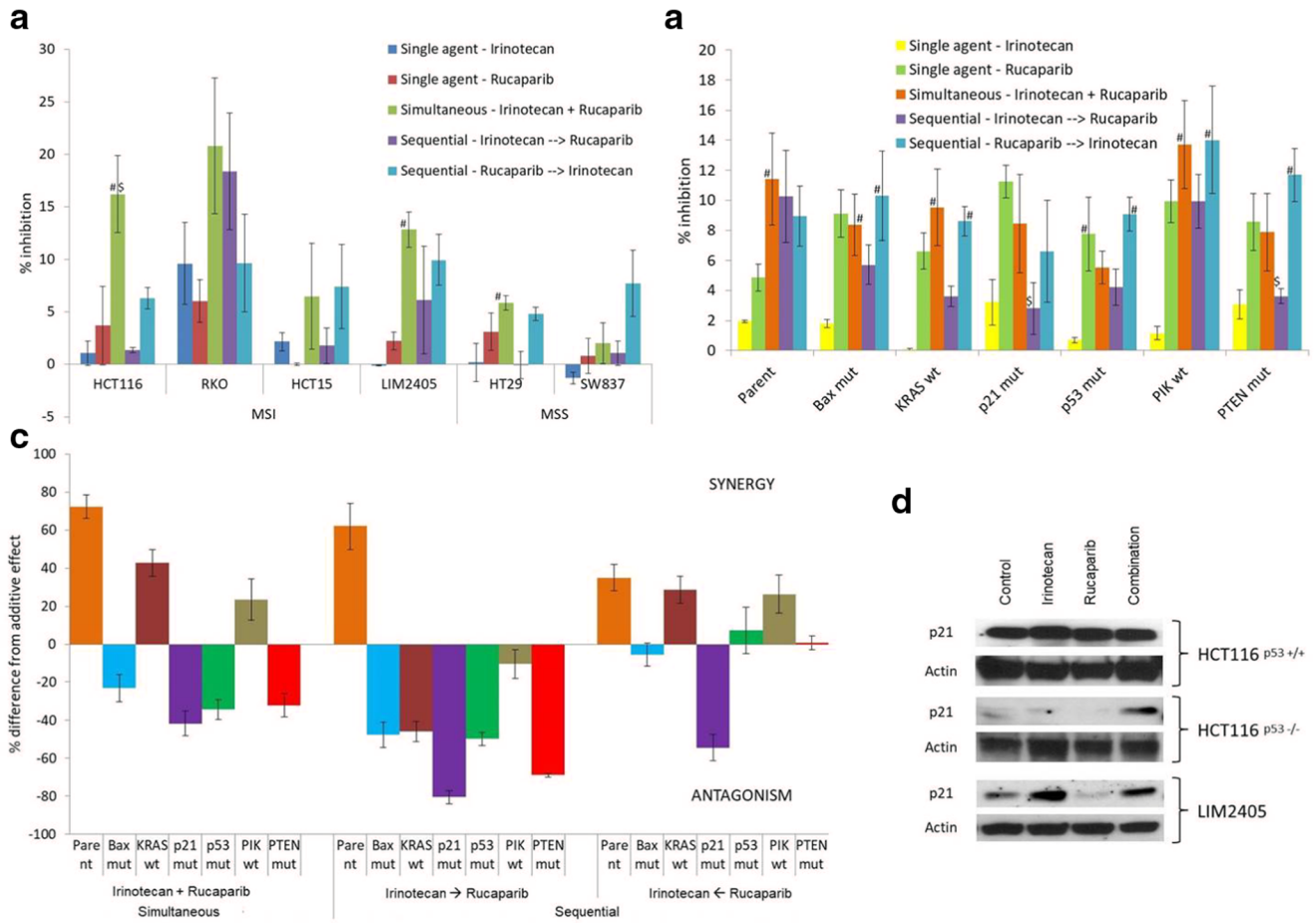


**Fig. 4 Effectiveness of simultaneous and sequence-dependent treatments of irinotecan and rucaparib in MSI (HCT116, RKO, HCT15 and LIM2405), MSS (HT29 and SW837) and six isogenic cell lines of HCT116.** Cells were treated with irinotecan, 200 nM and rucaparib, 400 nM for 24 h. Degree of cell death was inferred by SRB assay after 48 h of incubation. **a** Simultaneous treatment and administration of irinotecan prior to rucaparib were observed to be more cytotoxic in MSI cell lines. Administration of rucaparib prior to irinotecan led to significantly higher cytotoxicity as compared to simultaneous and vice versa treatments in SW837 (MSS). **b** Bax, p21, p53 and PTEN were most and mutational status of KRAS and PI3K were least important for eliciting synergy under simultaneous treatment. p53 is shown to be most important for the mechanism of irinotecan action. **c** Absence of Bax and p21 produced antagonism in HCT116 isogenic cell lines by any method of treatment. Each bar represents mean and SEM from 4 separate experiments. Statistical significance at $p \leq 0.05$ compared with * - control, $ - rucaparib and # - irinotecan. **d** Figure represents expression of p21 in isogenic HCT116 p53+/+ (p53 wt), HCT116 p53 −/− (p53-null) and LIM2405 upon treatment with irinotecan and rucaparib, 200 nM and 400 nM respective, for 24 h as seen in Western blots. Expression of p21 was drastically reduced upon treatment with rucaparib in p53 mutant and wt LIM2405 cell line

## Increase in growth inhibition of human colorectal carcinoma xenografts in mice following combined treatment

In order to confirm these in vitro findings, nude mice were injected with HCT116 and allowed to generate tumors. Irinotecan and rucaparib were administered alone or in combination for 2.5 weeks [28]. All treatments significantly reduced tumor size compared to control (Fig. 6a). Combination therapy resulted in a more significant reduction in tumor volume than single-agent groups. By day 17 of drug administration, the mean tumor volume of the combination treatment group was significantly smaller than that of either irinotecan-alone or rucaparib-alone groups ($p = 0.005$ vs irinotecan and $p = 0.007$ vs rucaparib). Indeed, in combination, the inhibitory ratio of tumor weight was 96%, while it was 80% and 79% in the irinotecan and rucaparib groups, respectively (Fig. 6b) [29]. No significant weight loss was observed before or after treatments in any of the cohorts (data not shown).

Immunohistochemical analyses of xenograft tumors demonstrated that expression of caspase 3, a marker of early apoptosis and activator of death protease, was increased upon treatment with rucaparib, irinotecan and their combination. Ki67, pancytokeratin and ribosomal protein S6 kinase beta-1 (RPS6KB1) were each significantly decreased in the combination treatment group as compared to control. These results suggest that combinatorial treatment suppressed tumor growth and differentiation by inhibiting cell proliferation and inducing cellular apoptosis in vivo. Absence of cytokeratin staining

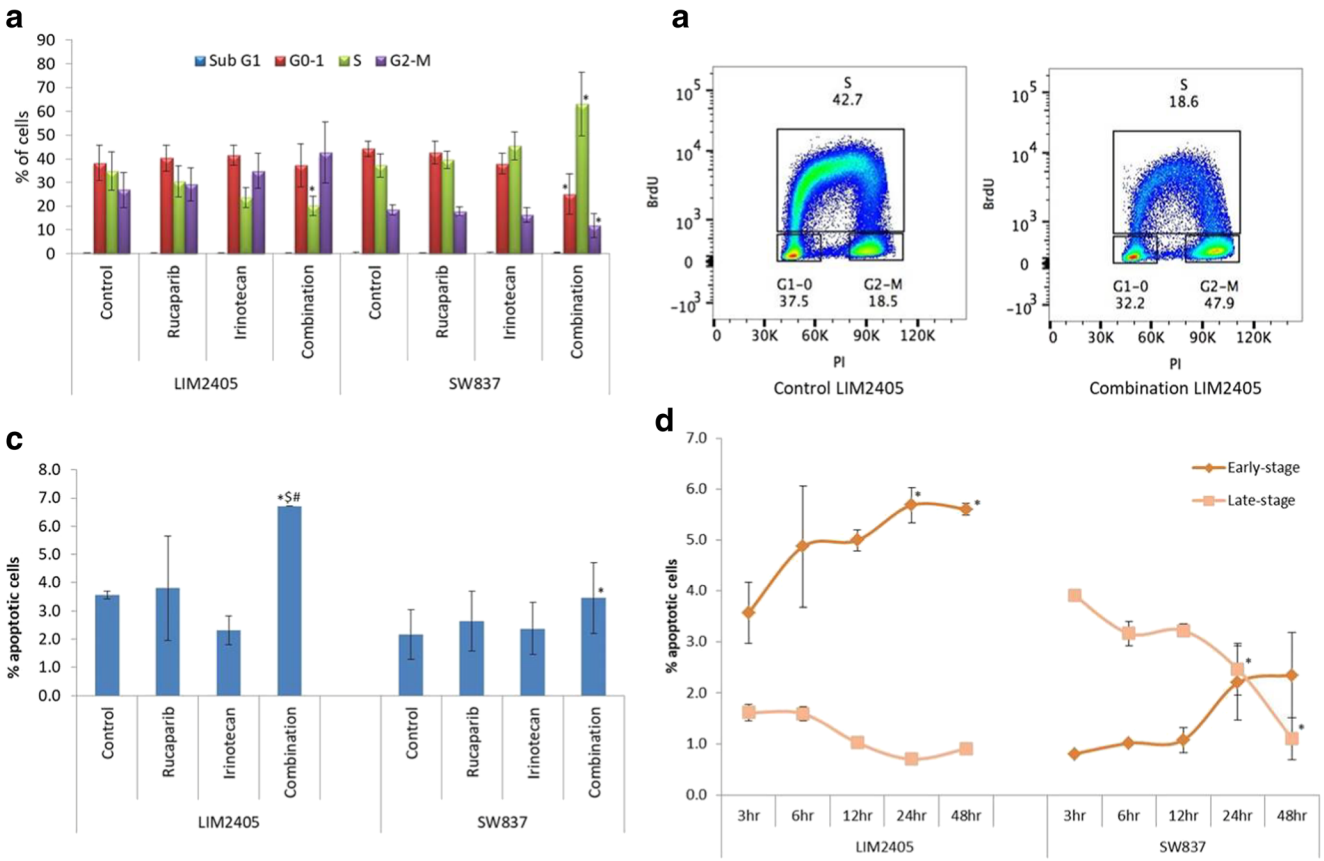


**Fig. 5 Cell cycle progression and apoptosis in MSS and MSI by flow cytometry.** LIM2405 (MSS) and SW837 were untreated or treated with irinotecan, rucaparib and combination. **a** Distribution and percentage of cells in pre-phase, G0–1, S and G2-M phase of the cell cycle are indicated. Combined treatment of irinotecan, 200 nM, and rucaparib, 400 nM, caused S phase arrest in SW837 and G2-M arrest in LIM2405 (**b**). Measurement of apoptosis is depicted in Fig. **c** and **d**. Cells were treated with rucaparib, irinotecan and combination for 3, 6, 12, 24 and 48 h and measured total and early- and late-stage apoptosis using Annexin V and PI stains under flow cytometry. **c** Figure provides percentage of total apoptotic cells upon 48 h of treatment. Combined treatment yielded significant levels of apoptosis in LIM2405, whereas in SW837, the combination did not produce significant apoptosis compared to single agents. **d** This figure shows percentage of early- and late-stage apoptotic cells in LIM2405 and SW837 upon combined treatment for 3–48 h. Early-stage apoptotic cells increased significantly in LIM2405 whereas late-stage increased in SW837 except for 48 h. Cells that are considered viable are both Annexin V and PI negative, while cells that are in early apoptosis are Annexin V positive and PI negative, and cells that are in late apoptosis or already dead are both Annexin V and PI positive. Each value represents mean ± SD of duplicate experiments. $p \leq 0.05$ (* - compared to control, $ - compared to rucaparib, # - compared to irinotecan) is considered as statistically significant

may be an indication of reduced cancer cell invasion and migration/metastasis. Reduced expression of RPS6KB1 has been shown to be an indication of diminished activity of mTOR (mammalian target of rapamycin) (Fig. 6c).

## Discussion

DNA repair inhibitors can improve the therapeutic index of chemotherapeutic drugs by targeting cancer cells over normal cells. A number of preclinical studies have demonstrated that PARP inhibitors can be potentially viable as chemopotentiators or chemo- and radio-sensitizers [30]. Although combining PARP inhibitors with a wide range of drugs is actively being pursued, it is critical to elucidate whether different PARP inhibitors should be considered equal and how such combinations work. Some PARP inhibitors selectively induce PARP-DNA trapping in addition to catalytic PARP inhibition [31]. By screening a collection of twelve combinations of DNA damaging/cytotoxic agents and small molecule PARP inhibitors, we identified one particular combination, irinotecan and rucaparib, which synergistically inhibited the growth of colorectal cancer cell lines and tumor/HCT116 xenografts in athymic nude mice. Our preclinical study demonstrates marked differences among combinations of established chemotherapeutic agents - oxaliplatin, 5-fluorouracil and irinotecan - with PARP inhibitors in advanced clinical development - olaparib, rucaparib, PJ34 and veliparib - which differ by their PARP-trapping efficiencies [11]. Here, we compared not only the combinations among themselves, but also with respective to single agent treatments. These interactions were tested and confirmed in multiple CRC cell lines. The platinum

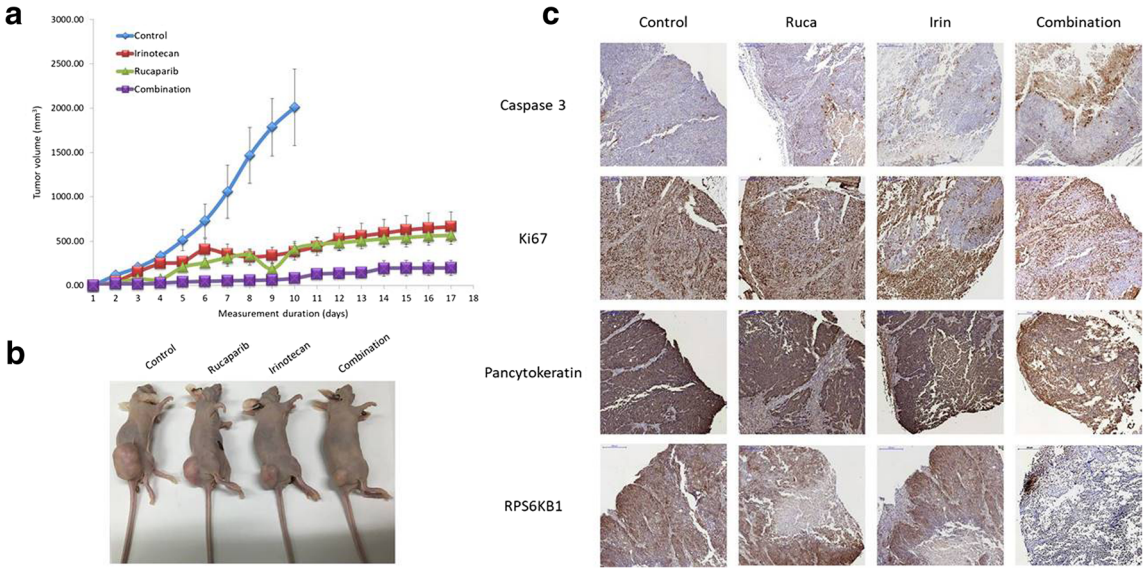


**Fig. 6 In vivo xenograft study. a** Line graph represents the results of HCT116 xenograft studies performed in athymic nude mice. Highly significant ($p = 0.005$) reduction in tumor volume was observed in mice treated with irinotecan and rucaparib. Each value is expressed as mean ± SD for 6 mice in each group. **b** Pictorial representation of reduction in tumor volume after treatment with agents for about 2 weeks. **c** Immunohistochemical staining for caspase 3, Ki67, pancytokeratin and RPS6KB1 (10x magnification) in HCT116 xenografted tissue. Caspase 3 was significantly increased, whereas Ki67, pancytokeratin and RPS6KB1 were reduced in expression in combinatorial treatment group. While some degree of caspase activity was seen in the single-agent treated groups also, there was no significant difference in expression of other proteins between controls and single-agent treated groups

analogues function by forming complex DNA adducts including intra-strand and inter-strand crosslinks [32]. Repair of these lesions is mediated by multiple DNA repair systems. The antagonism or lack of synergy between olaparib/rucaparib/veliparib and oxaliplatin might be explained by the fact that inhibition of PARP blocks only one of several repair pathways, and also fails to sensitize cells to these agents.

Topoisomerase inhibitors exert their cytotoxic effects by stabilizing and trapping the topoisomerase enzyme complex on the DNA, thereby preserving transient double-strand breaks or introducing new double-strand breaks from topoisomerase-mediated single-strand breaks during S phase of the cell cycle [33]. The broken 3′-DNA ends are covalently attached to topoisomerase I, whereas the 5′-DNA ends bear a sugar hydroxyl. The binding of PARP1 depends on the DNA substrate [34, 35]. PARP1 preferentially binds directly to base excision repair–intermediates with a 5′-2-deoxyribose-5-phosphate (5'-dRP) rather than to 5′-phosphate ends [36]. PARP is critical for the repair of topoisomerase I cleavage complexes [37]. PARylation can reverse topoisomerase I cleavage complexes [38], limit replication fork collisions, and facilitate homologous recombination at replication forks stalled by topoisomerase I cleavage complexes [11, 39]. This makes it logical for a combination of irinotecan and rucaparib to function most synergistically. Administration of rucaparib for 48 h significantly reduced irinotecan-induced PAR accumulation in tumors, which was more evident in the MSI cell line, LIM2405, compared to its MSS counterpart, SW837. The combinatorial effect was reflected in enhanced expression of γH2AX and dramatic cell cycle arrest. As a sensor of DNA damage signaling, γH2AX plays an important role in recruiting DDR proteins to the DNA lesion sites and initiating DDR, including activating cell cycle checkpoints [40].

G2-M arrest observed with irinotecan treatment was an added proof of the DNA damaging effect of the drug [41]. However, the effect was enhanced most prominently by the addition of rucaparib in the MSI cell line, LIM2405. In the face of DNA damage, cells arrest in G2-M to facilitate repair and although functional p53 is not required for this arrest, it is needed for cells to leave G2-M phase efficiently [42]. Irinotecan was shown to induce cell cycle arrest with a decrease in the proportion of cells in S and a relative increase in the percentage of cells in G2-M phase when given at $IC_{50}$ concentrations (250 nM) [43]. Active p53 facilitates cell cycle progression in the presence of DNA damage and this progression is inhibited by rucaparib. One possible explanation for this could be that p53 is PARylated in response to PARP activation, preventing nuclear export [44]. Thus, it is possible that the presence of the PARP inhibitor abrogates p53 PARylation preventing normal functionality. PARP has a number of diverse cellular functions including: regulation of cell survival and death pathways, transcription regulation, telomere cohesion, mitotic spindle formation, intracellular energy metabolism and trafficking of signaling proteins such as p53, p63 and NFκB [45, 46]. In this context PARylation prevents interaction of these molecules with exportin-1 (XPO-1), a mediator of nuclear export, and as such inhibits normal trafficking to the cytoplasm [47]. Our results are in keeping with that of others

that showed the PARP inhibitor, rucaparib, synergized with the topoisomerase I poisons topotecan and camptothecin and induced cell death via apoptosis [48]. Like many of the PARP inhibitors, rucaparib is an NAD+ analogue small molecule inhibitor of PARP and may function by preventing cross PARylation (PARylation of PARP by PARP) and subsequent release of PARP from DNA damage sites. As such DNA bound PARP would induce cell death by interfering with transcription and the progress of replication forks [6]. Here we report a synergistic effect for combined treatment of olaparib with irinotecan too; but, olaparib required higher concentration than that of rucaparib in order to exert synergy.

Our results indicate that combinatorial treatment remarkably increased the expression of cleaved caspase-3, which is activated by the upstream caspase-8 and caspase-9, and serves as a convergence point for different apoptosis signaling pathways [49]. Cleaved caspase-3 could inactivate PARP in turn, and thus eventually result in activation of the apoptotic cascade [50]. Increased Ki67, the nuclear antigen expressed in proliferating cells from G1 to M-phase of the cell cycle, is an independent good prognostic marker in CRC [51]. The role of combination of irinotecan and rucaparib in reducing the expression of Ki67 might be linked to cell cycle arrest as observed in S phase of SW837 or G2-M of LIM2405, or expression of p53 and β-catenin in regulating cell proliferation. β-Catenin is a key factor in Wingless Int-1 (WNT) signaling, and nuclear translocation of β-catenin characterizes cells with active WNT signaling. Active WNT signaling leads to enhanced cell proliferation and, thus, to elevated Ki67 [52]. We also examined the role of combination treatment in reducing the expression of RPS6KB1, a substrate of mammalian target of rapamycin (mTOR) that regulates cell proliferation [53]. Major mediators of mTOR function, the RAS/MAPK and PI3K/AKT pathways and PTEN loss are constitutively altered in CRC [54].

Besides factors that influence cell proliferation, biomarkers that play a critical role in regulating epithelial–mesenchymal transition (EMT) in cancer cells have been associated with poor prognosis or progressive disease in CRC [55]. Decreased expression of pan-cytokeratin, a commonly used epithelial cell marker, in the treated groups might be an indication of improved prognosis. Satelli et al. has suggested that detecting and measuring cell-surface vimentin on the surface of EMT-circulating tumor cells may predict progressive disease in CRC [55]. However, the relationship between regulation of WNT, mTOR and EMT pathways and combinatorial effect of irinotecan and rucaparib in reducing cell proliferation and inducing apoptosis need to be further elucidated.

This investigation is perhaps the first to demonstrate that not all PARPi are equal in exerting antitumor efficacy when combined with chemotherapeutic agents such as oxaliplatin, irinotecan and 5-fluorouracil. The combination of irinotecan and rucaparib for 48 h proved to be the optimal synergistic strategy based on the cytotoxic effect, the combination index and the levels and expression of PAR, PARP1 and γH2AX respectively. Cell cycle perturbations and percentage of cells appearing in total, early-and late-stage apoptosis in MSI over MSS cells improved upon combination treatment. Although observed differences between concurrent and sequential administration of irinotecan and rucaparib were not statistically significant in MSI, MSS and isogenic cells, rucaparib prior to irinotecan administration was more cytotoxic than the alternative sequence. Confirmative studies using animal models demonstrated that the combination of irinotecan and rucaparib is effective in nude mice bearing HCT116 xenografts, and the treatment strategy also led to the alteration in expression of key signaling proteins such as caspase 3, ki67, pancytokeratin and RPS6KB1.

The role of PARPi in the clinical setting is progressively gaining space and speed. The USFDA has currently approved 3 different PARPi, namely, olaparib, niraparib, and rucaparib, all for indications to treat ovarian cancer. The approval further mandates testing and confirmation of BRCA mutations as a biomarker for certain indications. Further, there are multiple clinical trials ongoing that are testing various PARPi, alone and in combination with cytotoxic chemotherapy. Preclinical studies exploring optimal utilization of these agents are essential to rational drug development. We have used a unique approach of testing multiple PARPi with the cytotoxic agents used in CRC, and demonstrated in both in vitro and in vivo models that an optimal precision approach appears to be combination irinotecan with rucaparib to treat CRC.

**Acknowledgements** S. Goel is supported by a K-12 award from the National Cancer Institute of the National Institutes of Health 1K12CA132783-01A1, and an Advanced Clinical Research Award (ACRA) in colon cancer, by the ASCO (now Conquer) Cancer Foundation. The authors would like to thank Dr. Tanya Dragic from Department of Microbiology & Immunology, Dr. Balazs Halmos from Department of Medicine and Dr. Thomas J. Ow from Department of Pathology, Albert Einstein College of Medicine/Montefiore Medical Center for their helpful advice on various technical issues examined in this paper, and Dr. Dhanonjoy C. Saha from Office of Grant Support, Albert Einstein College of Medicine, for his advice and comments. The authors also greatly appreciate the expert advice/assistance of Hillary Guzik, Analytical Imaging Facility, Albert Einstein College of Medicine in microscopy/IHC studies. The imaging was conducted in the Analytical Imaging Facility, which is funded by the NCI Cancer Grant P30CA013330.

**Funding** The work was supported by the K-12 award from the National Cancer Institute of the National Institutes of Health 1K12CA132783-01A1, and an Advanced Clinical Research Award (ACRA) in colon cancer, by the ASCO (now Conquer) Cancer Foundation to Dr. Sanjay Goel.

## Compliance with ethical standards

**Conflict of interest** Titto Augustine declares that he has no conflict of interest. Radhashree Maitra declares that she has no conflict of interest. Jinghang Zhang declares that she has no conflict of interest. Jay Nayak declares that he has no conflict of interest. Sanjay Goel declares that he has no conflict of interest.

**Ethical approval** This article does not contain any studies with human participants. All applicable institutional guidelines (by Institutional Animal Care and Use Committee) for the care and use of animals were followed.

## References


1. Lin YL, Liau JY, Yu SC, Ou DL, Lin LI, Tseng LH, Chang YL, Yeh KH, Cheng AL (2012) KRAS mutation is a predictor of oxaliplatin sensitivity in colon cancer cells. PLoS One 7(11):e50701. https://doi.org/10.1371/journal.pone.0050701
2. Peters GJ (2015) Therapeutic potential of TAS-102 in the treatment of gastrointestinal malignancies. Ther Adv Med Oncol 7(6):340–356. https://doi.org/10.1177/1758834015603313
3. Platell C, Ng S, O'Bichere A, Tebbutt N (2011) Changing management and survival in patients with stage IV colorectal cancer. Dis Colon Rectum 54(2):214–219. https://doi.org/10.1007/DCR.0b013e3182023bb0
4. Rabik CA, Dolan ME (2007) Molecular mechanisms of resistance and toxicity associated with platinating agents. Cancer Treat Rev 33(1):9–23. https://doi.org/10.1016/j.ctrv.2006.09.006
5. Osoegawa A, Gills JJ, Kawabata S, Dennis PA (2017) Rapamycin sensitizes cancer cells to growth inhibition by the PARP inhibitor olaparib. Oncotarget 8(50):87044–87053. https://doi.org/10.18632/oncotarget.19667
6. Wei H, Yu X (2016) Functions of PARylation in DNA damage repair pathways. Genomics Proteomics Bioinformatics 14(3):131–139. https://doi.org/10.1016/j.gpb.2016.05.001
7. Dizdar O, Arslan C, Altundag K (2015) Advances in PARP inhibitors for the treatment of breast cancer. Expert Opin Pharmacother 16(18):2751–2758. https://doi.org/10.1517/14656566.2015.1100168
8. Munoz-Gamez JA, Martin-Oliva D, Aguilar-Quesada R, Canuelo A, Nunez MI, Valenzuela MT, Ruiz de Almodovar JM, De Murcia G, Oliver FJ (2005) PARP inhibition sensitizes p53-deficient breast cancer cells to doxorubicin-induced apoptosis. Biochem J 386(Pt 1):119–125. https://doi.org/10.1042/BJ20040776
9. Walsh C (2018) Targeted therapy for ovarian cancer: the rapidly evolving landscape of PARP inhibitor use. Minerva Ginecol 70(2):150–170. https://doi.org/10.23736/S0026-4784.17.04152-1
10. Foucquier J, Guedj M (2015) Analysis of drug combinations: current methodological landscape. Pharmacol Res Perspect 3(3):e00149. https://doi.org/10.1002/prp2.149
11. Murai J, Zhang Y, Morris J, Ji J, Takeda S, Doroshow JH, Pommier Y (2014) Rationale for poly(ADP-ribose) polymerase (PARP) inhibitors in combination therapy with camptothecins or temozolomide based on PARP trapping versus catalytic inhibition. J Pharmacol Exp Ther 349(3):408–416. https://doi.org/10.1124/jpet.113.210146
12. Augustine TA, Baig M, Sood A, Budagov T, Atzmon G, Mariadason JM, Aparo S, Maitra R, Goel S (2015) Telomere length is a novel predictive biomarker of sensitivity to anti-EGFR therapy in metastatic colorectal cancer. Br J Cancer 112(2):313–318. https://doi.org/10.1038/bjc.2014.561
13. Gandhi JS, Goswami M, Sharma A, Tanwar P, Gupta G, Gupta N, Pasricha S, Mehta A, Singh S, Agarwal M, Gupta N (2017) Clinical impact of mismatch repair protein testing on outcome of early staged colorectal carcinomas. J Gastrointest Cancer 49:406–414. https://doi.org/10.1007/s12029-017-9954-5
14. Shirasawa S, Furuse M, Yokoyama N, Sasazuki T (1993) Altered growth of human colon cancer cell lines disrupted at activated Ki-ras. Science 260(5104):85–88
15. Samuels Y, Diaz LA Jr, Schmidt-Kittler O, Cummins JM, Delong L, Cheong I, Rago C, Huso DL, Lengauer C, Kinzler KW, Vogelstein B, Velculescu VE (2005) Mutant PIK3CA promotes cell growth and invasion of human cancer cells. Cancer Cell 7(6):561–573. https://doi.org/10.1016/j.ccr.2005.05.014
16. Jhawer M, Goel S, Wilson AJ, Montagna C, Ling YH, Byun DS, Nasser S, Arango D, Shin J, Klampfer L, Augenlicht LH, Perez-Soler R, Mariadason JM (2008) PIK3CA mutation/PTEN expression status predicts response of colon cancer cells to the epidermal growth factor receptor inhibitor cetuximab. Cancer Res 68(6):1953–1961. https://doi.org/10.1158/0008-5472.CAN-07-5659
17. Ross DT, Scherf U, Eisen MB, Perou CM, Rees C, Spellman P, Iyer V, Jeffrey SS, Van de Rijn M, Waltham M, Pergamenschikov A, Lee JC, Lashkari D, Shalon D, Myers TG, Weinstein JN, Botstein D, Brown PO (2000) Systematic variation in gene expression patterns in human cancer cell lines. Nat Genet 24(3):227–235. https://doi.org/10.1038/73432
18. Samaraweera L, Adomako A, Rodriguez-Gabin A, McDaid HM (2017) A novel indication for panobinostat as a senolytic drug in NSCLC and HNSCC. Sci Rep 7(1):1900. https://doi.org/10.1038/s41598-017-01964-1
19. Chou TC (2010) Drug combination studies and their synergy quantification using the Chou-Talalay method. Cancer Res 70(2):440–446. https://doi.org/10.1158/0008-5472.CAN-09-1947
20. Qin Y, Qi N, Tang Y, He J, Li X, Gu F, Zou S (2015) Isolation and identification of a high molecular weight protein in sow milk. Animal 9(5):847–854. https://doi.org/10.1017/S1751731114003280
21. Palma JP, Rodriguez LE, Bontcheva-Diaz VD, Bouska JJ, Bukofzer G, Colon-Lopez M, Guan R, Jarvis K, Johnson EF, Klinghofer V, Liu X, Olson A, Saltarelli MJ, Shi Y, Stavropoulos JA, Zhu GD, Penning TD, Luo Y, Giranda VL, Rosenberg SH, Frost DJ, Donawho CK (2008) The PARP inhibitor, ABT-888 potentiates temozolomide: correlation with drug levels and reduction in PARP activity in vivo. Anticancer Res 28(5A):2625–2635
22. Brookes S, Gagrica S, Sanij E, Rowe J, Gregory FJ, Hara E, Peters G (2015) Evidence for a CDK4-dependent checkpoint in a conditional model of cellular senescence. Cell Cycle 14(8):1164–1173. https://doi.org/10.1080/15384101.2015.1010866
23. Vermes I, Haanen C, Reutelingsperger C (2000) Flow cytometry of apoptotic cell death. J Immunol Methods 243(1–2):167–190
24. He BC, Gao JL, Luo X, Luo J, Shen J, Wang L, Zhou Q, Wang YT, Luu HH, Haydon RC, Wang CZ, Du W, Yuan CS, He TC, Zhang BQ (2011) Ginsenoside Rg3 inhibits colorectal tumor growth through the down-regulation of Wnt/ss-catenin signaling. Int J Oncol 38(2):437–445. https://doi.org/10.3892/ijo.2010.858
25. Xiao K, Luo J, Fowler WL, Li Y, Lee JS, Xing L, Cheng RH, Wang L, Lam KS (2009) A self-assembling nanoparticle for paclitaxel delivery in ovarian cancer. Biomaterials 30(30):6006–6016. https://doi.org/10.1016/j.biomaterials.2009.07.015
26. Zhao E, Ilyas G, Cingolani F, Choi JH, Ravenelle F, Tanaka KE, Czaja MJ (2017) Pentamidine blocks hepatotoxic injury in mice. Hepatology 66(3):922–935. https://doi.org/10.1002/hep.29244
27. Hammond WA, Swaika A, Mody K (2016) Pharmacologic resistance in colorectal cancer: a review. Ther Adv Med Oncol 8(1):57–84. https://doi.org/10.1177/1758834015614530
28. Bradshaw-Pierce EL, Pitts TM, Kulikowski G, Selby H, Merz AL, Gustafson DL, Serkova NJ, Eckhardt SG, Weekes CD (2013) Utilization of quantitative in vivo pharmacology approaches to assess combination effects of everolimus and irinotecan in mouse xenograft models of colorectal cancer. PLoS One 8(3):e58089. https://doi.org/10.1371/journal.pone.0058089
29. Tsukihara H, Nakagawa F, Sakamoto K, Ishida K, Tanaka N, Okabe H, Uchida J, Matsuo K, Takechi T (2015) Efficacy of combination chemotherapy using a novel oral chemotherapeutic agent, TAS-102, together with bevacizumab, cetuximab, or panitumumab on human colorectal cancer xenografts. Oncol Rep 33(5):2135–2142. https://doi.org/10.3892/or.2015.3876

30. Vormoor B, Curtin NJ (2014) Poly(ADP-ribose) polymerase inhibitors in Ewing sarcoma. Curr Opin Oncol 26(4):428–433. https://doi.org/10.1097/CCO.0000000000000091
31. Murai J, Huang SY, Das BB, Renaud A, Zhang Y, Doroshow JH, Ji J, Takeda S, Pommier Y (2012) Trapping of PARP1 and PARP2 by clinical PARP inhibitors. Cancer Res 72(21):5588–5599. https://doi.org/10.1158/0008-5472.CAN-12-2753
32. Noll DM, Mason TM, Miller PS (2006) Formation and repair of interstrand cross-links in DNA. Chem Rev 106(2):277–301. https://doi.org/10.1021/cr040478b
33. Nicolay NH, Ruhle A, Perez RL, Trinh T, Sisombath S, Weber KJ, Schmezer P, Ho AD, Debus J, Saffrich R, Huber PE (2016) Mesenchymal stem cells exhibit resistance to topoisomerase inhibition. Cancer Lett 374(1):75–84. https://doi.org/10.1016/j.canlet.2016.02.007
34. Abdou I, Poirier GG, Hendzel MJ, Weinfeld M (2015) DNA ligase III acts as a DNA strand break sensor in the cellular orchestration of DNA strand break repair. Nucleic Acids Res 43(2):875–892. https://doi.org/10.1093/nar/gku1307
35. Stewart E, Goshorn R, Bradley C, Griffiths LM, Benavente C, Twarog NR, Miller GM, Caufield W, Freeman BB 3rd, Bahrami A, Pappo A, Wu J, Loh A, Karlstrom A, Calabrese C, Gordon B, Tsurkan L, Hatfield MJ, Potter PM, Snyder SE, Thiagarajan S, Shirinifard A, Sablauer A, Shelat AA, Dyer MA (2014) Targeting the DNA repair pathway in Ewing sarcoma. Cell Rep 9(3):829–841. https://doi.org/10.1016/j.celrep.2014.09.028
36. Cao TP, Kim JS, Woo MH, Choi JM, Jun Y, Lee KH, Lee SH (2016) Structural insight for substrate tolerance to 2-deoxyribose-5-phosphate aldolase from the pathogen Streptococcus suis. J Microbiol 54(4):311–321. https://doi.org/10.1007/s12275-016-6029-4
37. Strumberg D, Pilon AA, Smith M, Hickey R, Malkas L, Pommier Y (2000) Conversion of topoisomerase I cleavage complexes on the leading strand of ribosomal DNA into 5′-phosphorylated DNA double-strand breaks by replication runoff. Mol Cell Biol 20(11):3977–3987
38. Malanga M, Althaus FR (2004) Poly(ADP-ribose) reactivates stalled DNA topoisomerase I and induces DNA strand break resealing. J Biol Chem 279(7):5244–5248. https://doi.org/10.1074/jbc.C300437200
39. Sugimura K, Takebayashi S, Taguchi H, Takeda S, Okumura K (2008) PARP-1 ensures regulation of replication fork progression by homologous recombination on damaged DNA. J Cell Biol 183(7):1203–1212. https://doi.org/10.1083/jcb.200806068
40. Marechal A, Zou L (2013) DNA damage sensing by the ATM and ATR kinases. Cold Spring Harb Perspect Biol 5(9). https://doi.org/10.1101/cshperspect.a012716
41. Kaku Y, Tsuchiya A, Kanno T, Nishizaki T (2015) Irinotecan induces cell cycle arrest, but not apoptosis or necrosis, in Caco-2 and CW2 colorectal cancer cell lines. Pharmacology 95(3–4):154–159. https://doi.org/10.1159/000381029
42. Williams AB, Schumacher B (2016) p53 in the DNA-damage-repair process. Cold Spring Harb Perspect Med 6(5). https://doi.org/10.1101/cshperspect.a026070
43. Origanti S, Cai SR, Munir AZ, White LS, Piwnica-Worms H (2013) Synthetic lethality of Chk1 inhibition combined with p53 and/or p21 loss during a DNA damage response in normal and tumor cells. Oncogene 32(5):577–588. https://doi.org/10.1038/onc.2012.84
44. Abd Elmageed ZY, Naura AS, Errami Y, Zerfaoui M (2012) The poly(ADP-ribose) polymerases (PARPs): new roles in intracellular transport. Cell Signal 24(1):1–8. https://doi.org/10.1016/j.cellsig.2011.07.019
45. Davidson D, Wang Y, Aloyz R, Panasci L (2013) The PARP inhibitor ABT-888 synergizes irinotecan treatment of colon cancer cell lines. Investig New Drugs 31(2):461–468. https://doi.org/10.1007/s10637-012-9886-7
46. Lieberman HB, Panigrahi SK, Hopkins KM, Wang L, Broustas CG (2017) p53 and RAD9, the DNA damage response, and regulation of transcription networks. Radiat Res 187(4):424–432. https://doi.org/10.1667/RR003CC.1
47. Rosado MM, Bennici E, Novelli F, Pioli C (2013) Beyond DNA repair, the immunological role of PARP-1 and its siblings. Immunology 139(4):428–437. https://doi.org/10.1111/imm.12099
48. Lee YC, Lee CH, Tsai HP, An HW, Lee CM, Wu JC, Chen CS, Huang SH, Hwang J, Cheng KT, Leiw PL, Chen CL, Lin CM (2015) Targeting of topoisomerase I for prognoses and therapeutics of camptothecin-resistant ovarian cancer. PLoS One 10(7):e0132579. https://doi.org/10.1371/journal.pone.0132579
49. Huang K, Zhang J, O'Neill KL, Gurumurthy CB, Quadros RM, Tu Y, Luo X (2016) Cleavage by caspase 8 and mitochondrial membrane association activate the BH3-only protein bid during TRAIL-induced apoptosis. J Biol Chem 291(22):11843–11851. https://doi.org/10.1074/jbc.M115.711051
50. McIlwain DR, Berger T, Mak TW (2015) Caspase functions in cell death and disease. Cold Spring Harb Perspect Biol 7(4). https://doi.org/10.1101/cshperspect.a026716
51. Mao D, Qiao L, Lu H, Feng Y (2016) B-cell translocation gene 3 overexpression inhibits proliferation and invasion of colorectal cancer SW480 cells via Wnt/beta-catenin signaling pathway. Neoplasma 63(5):705–716. https://doi.org/10.4149/neo_2016_507
52. Melling N, Kowitz CM, Simon R, Bokemeyer C, Terracciano L, Sauter G, Izbicki JR, Marx AH (2016) High Ki67 expression is an independent good prognostic marker in colorectal cancer. J Clin Pathol 69(3):209–214. https://doi.org/10.1136/jclinpath-2015-202985
53. Al-Ali H, Ding Y, Slepak T, Wu W, Sun Y, Martinez Y, Xu XM, Lemmon VP, Bixby JL (2017) The mTOR substrate S6 kinase 1 (S6K1) is a negative regulator of axon regeneration and a potential drug target for central nervous system injury. J Neurosci 37(30):7079–7095. https://doi.org/10.1523/JNEUROSCI.0931-17.2017
54. Therkildsen C, Bergmann TK, Henrichsen-Schnack T, Ladelund S, Nilbert M (2014) The predictive value of KRAS, NRAS, BRAF, PIK3CA and PTEN for anti-EGFR treatment in metastatic colorectal cancer: a systematic review and meta-analysis. Acta Oncol 53(7):852–864. https://doi.org/10.3109/0284186X.2014.895036
55. Satelli A, Mitra A, Brownlee Z, Xia X, Bellister S, Overman MJ, Kopetz S, Ellis LM, Meng QH, Li S (2015) Epithelial-mesenchymal transitioned circulating tumor cells capture for detecting tumor progression. Clin Cancer Res 21(4):899–906. https://doi.org/10.1158/1078-0432.CCR-14-0894